Atmospheric Pollution Research 5 (2014) 759-768



Atmospheric Pollution Research

www.atmospolres.com

The 2013 severe haze over the Southern Hebei, China: $PM_{2.5}$ composition and source apportionment

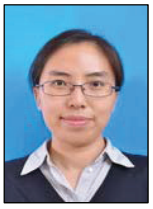
Zhe Wei [1], Li–Tao Wang [1], Ming–Zhang Chen [2], Yan Zheng [3]

[1] *Department of Environmental Engineering, School of City Construction, Hebei University of Engineering, Handan, Hebei 056038, China*
[2] *School of Civil Engineering, Shijiazhuang Railway Institute, No. 17 North 2nd–Ring East Road, Shijiazhuang, Hebei 050043, China*
[3] *The Environmental Monitoring Center of Handan, Handan, Hebei 056002, China*

ABSTRACT

$PM_{2.5}$ samples were collected and analyzed for the first time in Handan City, which was listed in the top 4 polluted cities in China, during December 2012 to January 2013 when the record–breaking severe haze pollution happened. Positive Matrix Factorization method (PMF) was applied to understand major sources to the severe haze pollution over this city. The daily average concentration of $PM_{2.5}$ was 160.1 μg m^{-3}, which was 2.1 times of the National Ambient Air Quality Standards of China (Class II, Annual Average Level) for daily average $PM_{2.5}$ of 75 μg m^{-3}. SO_4^{2-} was the most abundant ion (15.4%), followed by NH_4^+ and NO_3^-. They accounted for 39.5% of $PM_{2.5}$. Eight factors were identified by positive matrix factorization (PMF) model. The major sources were coal combustion source (25.9%), secondary source (21.8%), industry source (16.2%), Ba, Mn and Zn source (12.7%), motor vehicle source (7.7%), road dust source (10.9%), K^+, As and V source (6.3%) and fuel oil combustion source (2.5%).The mean value of extinction coefficient (B_{ext}) was 682.1 Mm^{-1} and the largest contributor to B_{ext} was ammonium sulfate with the mean value of 221.0 Mm^{-1}, accounted for 32.4% of the B_{ext}.

Keywords: *$PM_{2.5}$, OC, B_{ext}, PMF, source apportionment*



Corresponding Author:
Li–Tao Wang
☎ : *+86-310-8578755*
☏ : *+86-310-8578755*
✉ : *wlt@tsinghua.edu.cn*

Article History:
Received: 07 February 2014
Revised: 06 June 2014
Accepted: 08 June 2014

doi: 10.5094/APR.2014.085

1. Introduction

Extremely severe, widespread haze occurred in Central and Eastern China during January 2013. The haze event attracted a wide attention locally and worldwide, because the haze in this month was the most serious pollution episode since 1961. According to the statistics published by the Ministry of Environmental Protection for January 2013, the top ten polluted cities are Xingtai, Shijiazhuang, Baoding, Handan, Langfang, Hengshui, Jinan, Tangshan, Beijing and Zhengzhou, seven of which are within Hebei.

Very few studies were pursued to study the characteristics of particulate matter in Handan, especially for fine particles. In the recent studies, Wang et al. (2012), Wei et al. (2013) and Wang et al. (2014) applied the CMAQ model and used the so–called "Brute Force" method (BFM) (Dunker et al., 1996) to simulate the air pollution over the southern Hebei cities and address the major sources of $PM_{2.5}$. Wang et al. (2012) and Wang et al. (2014) found that local sources contributed 64.2% to $PM_{2.5}$ in Handan in December 2007, 69.2% in January and 63.0% in February, 2013, respectively. However, to the best of our knowledge, there is no research focusing on the chemical components of $PM_{2.5}$ in Handan City. In this study, we sampled and analyzed $PM_{2.5}$ during the most polluted period in Handan and applied PMF, a widely implied receptor model, to indentify source apportionment of $PM_{2.5}$, to support the policy–making in air pollution control in this city.

2. Experimental and Analysis Methodology

2.1. Sampling

Handan is located in the intersection area of Hebei, Shanxi, Henan, and Shandong. The sampling site is located on the top of a 12–m high building at School of City Construction, Hebei University of Engineering (Figure 1). The sampling period was from December 1, 2012 to January 31, 2013. Daily $PM_{2.5}$ samples were collected continuously from 8:00 am to 7:30 am of the next day using a High Volume $PM_{2.5}$ air sampler (Thermo Scientific Co.) with 20.3 × 25.4 cm quartz filters (0.2 μm of pore size). Flow rate was 1.13 m^3 min^{-1} and a total of 55 samples were collected.

2.2. Chemical components analysis

Ionic analyses. A circular portion of the quartz filter (1 cm^2) was extracted into 10 mL ultrapure water (18.2 MΩ cm) to determine the concentration of water–soluble inorganic ions. The extracted solution was filtered through a microporous membrane filter (0.45 μm of pore size), and stored in a refrigerator at –18 °C until chemical analysis. An ion chromatograph (Dionex, DX–600, USA) was used to measure the water–soluble cations. Another ion chromato-graph (Dionex, ICS–2100, USA) was used to measure water–soluble anions.

Carbon analysis. The total carbon, organic carbon and element carbon were analyzed in Tsinghua University through methodology of TOR used Thermal/Optical Carbon Analyzer (Model 2001A) that

© Author(s) 2014. This work is distributed under the Creative Commons Attribution 3.0 License.

was produced by Desert Research Institute (DRI). A piece of processed sample filter (0.53 cm^2) was placed in an environment with pure He gas without O_2, and was heated progressively at 140 °C, 280 °C, 480 °C, and 580 °C, first to determine organic carbon contents OC1, OC2, OC3, and OC4, respectively. Then, in an environment with 2% O_2 and 98% He, the sample was further heated progressively at 580 °C, 740 °C, and 840 °C to determine the elemental carbon contents EC1, EC2, and EC3.

Elemental analyses. This study used ICP–MS to analyze the concentrations of trace elements (i.e., Ti, V, Cr, Mn, Ni, Cu, Zn, As, Se, Sr, Cd, Ba and Pb). A piece of filter (1 cm^2) was digested for 25 min at 190 °C with 8 mL concentrated nitric acid (BV–III) and 0.5 mL H_2O_2 (30%) in a Teflon microwave digestion tank (CEM, MARS). Then, the bulk solution was moved into a 100 mL flask. High–purity water was used to make up the volume. Finally, 10 mL solution was centrifuged for 10 min to remove any suspended solids before instrumental analyses.

2.3. Quality Assurance/Quality Control (QA/QC)

Sampling and weighing. There were several low–rise buildings around the sampling site. There was not a big emission source in this area. To ensure the flow of 1.13 m^3 min^{-1}, flow of the sampling equipment was checked every month. The silicone oil was replaced every 15 days to ensure the sampling rate of $PM_{2.5}$. These quartz filters were baked at 450 °C for 4 hours. Then, filters were put in a chamber at 25 °C and 50% of relatively humidity for 24 h until sampling. These sampled filters were put in the same chamber for 24 h until the second weigh. Then, filters were preserved in a refrigerator that set at –20 °C. All procedures were strictly quality controlled to avoid any possible contamination of the samples.

The sampling method was found to be effective since the measured concentrations agreed well with those measured using TEOM 1405D. In this period, three blank filters were preserved under the same environment were analyzed to guarantee the accuracy and reliability of sampling. The calculated concentrations for the blank filters were used to adjust the concentrations of the measured compositions.

Ionic analyses and carbon analysis. Glass containers were washed, and soaked in ultrapure water for over 24 h. Then, they were cleaned with supersonic waves for 45 min and were washed two times with ultrapure water (18.2 MΩ cm). The method detection limit (MDL) of NH_4^+, Na^+, K^+, Mg^{2+}, Ca^{2+}, SO_4^{2-}, Cl^-, NO_2^- and NO_3^- were 0.01, 0.001, 0.001, 0.004, 0.005, 0.01, 0.005, 0.01 and 0.01 μg mL^{-1}, respectively. The precision was <5% for TC and <10% for OC and EC. The MDL was 0.82 μg cm^{-2} for TOC and 0.20 μg cm^{-2} for TEC, respectively.

Elemental analyses. ICP–MS was calibrated by standard injection (r^2>0.99) and the samples were analyzed in triplicate. Relative standard deviation was kept below 5%. Internal standard recovery was controlled at the range from 80% to 120%.

2.4. Positive Matrix Factorization (PMF)

PMF is a multivariate factor analysis tool that decomposes a matrix of speciated sample data into two matrices, factor contributions and factor profiles, which then need to be interpreted by an analyst as to what source types are represented using measured source profile information, wind direction analysis, and emission inventories (U.S. EPA, 2008). The method is described in greater detail by Paatero and Tapper (1994) and Paatero (1997). PMF has been successfully applied to identify the pollutant sources (Lee et al., 1999; Chueinta et al., 2000; Qin et al., 2006; Brown et al., 2007; Kim and Hopke, 2008; Yang et al., 2013).

The brief principle is described in the following: A speciated data set can be viewed as a data matrix X of n by m dimensions, in which n is the number of samples and m is the number of chemical species measured. So $X=GF+E$, $G=n\times p$ and $F=p\times m$, where p is the number of pollutant sources, G is the matrix of source contribution, F is the matrix of species profile, and E is the residual matrix for each sample/species. The goal of PMF is to identify the number of pollutant sources F and G [see Equations (1)–(3)]. The PMF solution minimizes the object function Q [Equation (3)], based upon the uncertainties (u). Then PMF could calculate the G and F. The product of G and F can explain the systematic variations in X.

$$X_{ij} = \sum_{k=1}^{p} g_{ik} f_{kj} + e_{ij} \quad (1)$$

$$e_{ij} = X_{ij} - \sum_{k=1}^{p} g_{ik} f_{kj} \quad (2)$$

$$Q = \sum_{i=1}^{n} \sum_{j=1}^{m} [e_{ij}/u_{ij}] \quad (3)$$



Figure 1. *Location of the sampling site in Handan city (▲ indicates Hebei University of Engineering, and * indicates the sampling site).*

In this study, USEPA PMF 3.0 was used to analyze the source apportionment. The 10% of concentrations was used as the uncertainty of each species in the data set. If the concentration was less than or equal to MDL provided, 1/2 MDL was used to replace the concentration, the uncertainty was calculated using 5/6 MDL. Signal to noise (S/N) [see Equation (4), X_{ij} is the concentration of the j^{th} component in the i^{th} sampling day, S_{ij} is the standard deviation of X_{ij}] was used to review the dataset. The dataset was used directly when S/N exceeded 2. The results showed that the smallest value of S/N was 6.90 of Ti. Therefore, we considered that the dataset was reliable.

$$S/N = 0.5\left[\sum_{i=1}^{n}(X_{ij})^2 / \sum_{i=1}^{n}(S_{ij})^2\right]^{0.5} \quad (4)$$

Among these measured compositions, 23 species were selected to run the model except that NO_2^- and Ti. We run the model with 5 to 12 factors to explore the best solution. An eight–factor solution gave the most interpretable and reproducible results within the iterations tested. Scaled residuals were inspected, and 95.6% were between –3 and 3 for all of the species.

3. Results and Discussion

3.1. Chemical compositions of $PM_{2.5}$

Table 1 illustrated the concentrations and chemical components of $PM_{2.5}$ in different periods. The daily average concentration of $PM_{2.5}$ was 160.1 μg m^{-3} during this period. The daily average concentrations of $PM_{2.5}$ in December and January were 135.1 μg m^{-3} and 190.1 μg m^{-3}, which are 1.8 and 2.5 times of the daily $PM_{2.5}$ limit value (75 μg m^{-3}) set by the National Ambient Air Quality Standard in China (CNAAQS) (MEP, 2012), respectively.

In Wei et al. (2014) study, there was a typical pollution episode during January 2013. The present study was conducted to better understand the different characteristics and detailed components of particles before and after the episode. Table 1 presents the detailed concentrations measured between January 1–13 and January 14–31.

Water–soluble ions in $PM_{2.5}$. In this period, water–soluble ions contributed 48.3% to $PM_{2.5}$; almost a half of $PM_{2.5}$ suggesting that water–soluble ions are the major fraction in $PM_{2.5}$. Additionally, water–soluble ions contributed 54.6% and 42.9% to $PM_{2.5}$ in December and January, respectively. The proportion of December was higher than January. It implied that the proportion of water–soluble ions didn't increase along with increase of absolute concentration of $PM_{2.5}$. The proportions of January 1–13 and January 14–31 were 29.1% and 65.3%, respectively. It indicated that the proportion of water–soluble ions increased after the peak of the episode. The sum of SO_4^{2-}, NH_4^+ and NO_3^- accounted for 39.5%, 42.3% and 37.2% of $PM_{2.5}$ during this period, December and January, respectively. They were the major contributors to water–soluble ions. The proportion of January 1–13 was 23.3% while the proportion of January 14–31 was 58.6%. That was to say, in the early stage of episode, there were less water–soluble pollutants in the atmosphere.

Table 1. *Average concentrations of chemical components in $PM_{2.5}$ during December 2012 to January 2013*

	Mean Value (μg m^{-3})					S.D.[a] (μg m^{-3})				
	Whole Period	December	January	1–13	14–31	Whole Period	December	January	1–13	14–31
$PM_{2.5}$	160.1	135.1	190.1	217.7	139.5	77.9	57.2	89.4	139.5	41.1
OC	26.3	22.7	30.6	38.6	26.1	12.0	8.9	13.9	19.5	6.8
SO_4^{2-}	24.6	23.1	26.4	17.0	31.6	14.6	15.0	14.2	12.1	12.8
NH_4^+	19.9	17.4	22.9	18.9	25.1	9.1	8.5	9.0	10.0	7.8
NO_3^-	18.8	16.6	21.4	14.9	25.0	9.4	8.1	10.3	9.2	9.3
EC	15.8	16.8	14.7	20.1	11.6	7.3	6.8	7.9	10.5	3.6
Cl^-	9.2	4.8	10.9	9.0	6.0	7.1	5.1	3.6	4.2	2.7
K^+	2.4	1.1	2.6	2.4	2.1	2.2	1.2	1.0	1.4	0.8
Na^+	1.3	1.7	0.9	0.9	1.0	0.7	0.6	0.5	0.3	0.6
Ca^{2+}	0.9	1.3	0.4	0.8	0.2	0.9	1.1	0.4	0.5	0.1
Pb	0.3	0.2	0.3	0.3	0.3	0.2	0.2	0.2	0.2	0.1
Zn	0.3	0.3	0.3	0.3	0.3	0.2	0.2	0.2	0.3	0.1
NO_2^-	88.0×10^{-3}	142.3×10^{-3}	40.4×10^{-3}	0.6×10^{-3}	226.5×10^{-3}	153.1×10^{-3}	102.6×10^{-3}	154.8×10^{-3}	50.9×10^{-3}	146.9×10^{-3}
Mg^{2+}	125.2×10^{-3}	153.5×10^{-3}	91.2×10^{-3}	120.0×10^{-3}	75.1×10^{-3}	82.7×10^{-3}	98.1×10^{-3}	39.6×10^{-3}	35.5×10^{-3}	32.7×10^{-3}
As	21.4×10^{-3}	16.4×10^{-3}	27.5×10^{-3}	26.0×10^{-3}	28.3×10^{-3}	17.7×10^{-3}	13.8×10^{-3}	20.1×10^{-3}	24.4×10^{-3}	18.1×10^{-3}
Ba	10.1×10^{-3}	10.1×10^{-3}	10.1×10^{-3}	16.7×10^{-3}	6.3×10^{-3}	11.3×10^{-3}	12.2×10^{-3}	10.5×10^{-3}	14.5×10^{-3}	4.8×10^{-3}
Cd	4.3×10^{-3}	3.4×10^{-3}	5.3×10^{-3}	4.9×10^{-3}	5.5×10^{-3}	2.7×10^{-3}	2.1×10^{-3}	3.0×10^{-3}	4.1×10^{-3}	2.2×10^{-3}
Cr	8.2×10^{-3}	7.2×10^{-3}	9.4×10^{-3}	8.3×10^{-3}	9.9×10^{-3}	4.8×10^{-3}	4.5×10^{-3}	4.9×10^{-3}	6.7×10^{-3}	3.7×10^{-3}
Cu	18.8×10^{-3}	13.2×10^{-3}	25.4×10^{-3}	18.7×10^{-3}	29.2×10^{-3}	13.6×10^{-3}	10.8×10^{-3}	13.9×10^{-3}	15.8×10^{-3}	11.5×10^{-3}
Mn	67.6×10^{-3}	62.6×10^{-3}	73.4×10^{-3}	96.4×10^{-3}	60.6×10^{-3}	39.0×10^{-3}	1.7×10^{-3}	45.3×10^{-3}	65.7×10^{-3}	22.2×10^{-3}
Ni	3.4×10^{-3}	2.7×10^{-3}	4.2×10^{-3}	3.5×10^{-3}	4.6×10^{-3}	3.5×10^{-3}	1.7×10^{-3}	4.7×10^{-3}	2.4×10^{-3}	5.6×10^{-3}
Se	10.6×10^{-3}	9.0×10^{-3}	12.6×10^{-3}	14.8×10^{-3}	11.4×10^{-3}	6.3×10^{-3}	4.8×10^{-3}	7.4×10^{-3}	11.2×10^{-3}	4.1×10^{-3}
Sr	6.4×10^{-3}	7.4×10^{-3}	5.2×10^{-3}	6.9×10^{-3}	4.2×10^{-3}	6.3×10^{-3}	7.5×10^{-3}	4.1×10^{-3}	5.4×10^{-3}	2.9×10^{-3}
Ti	15.1×10^{-3}	65.7×10^{-3}	11.0×10^{-3}	8.9×10^{-3}	12.2×10^{-3}	20.3×10^{-3}	0.2×10^{-3}	14.6×10^{-3}	19.0×10^{-3}	12.1×10^{-3}
V	5.4×10^{-3}	5.7×10^{-3}	5.0×10^{-3}	5.3×10^{-3}	4.8×10^{-3}	5.9×10^{-3}	4.7×10^{-3}	7.1×10^{-3}	7.1×10^{-3}	7.4×10^{-3}

[a] *Standard deviation*

SO_4^{2-} was the most abundant ion in this period, its concentration ranged from 5.3 μg m^{-3} to 73.3 μg m^{-3} with an average of 24.6 μg m^{-3} as shown in Figure 2. It accounted for 15.4% of $PM_{2.5}$ and approximately 31.8% of the all measured ions. The average concentrations of NO_3^- and NH_4^+ were 18.8 μg m^{-3} and 19.9 μg m^{-3}, respectively. They accounted for 11.7% and 12.4% of $PM_{2.5}$ 24.3% and 25.7% of the all measured ions, respectively.

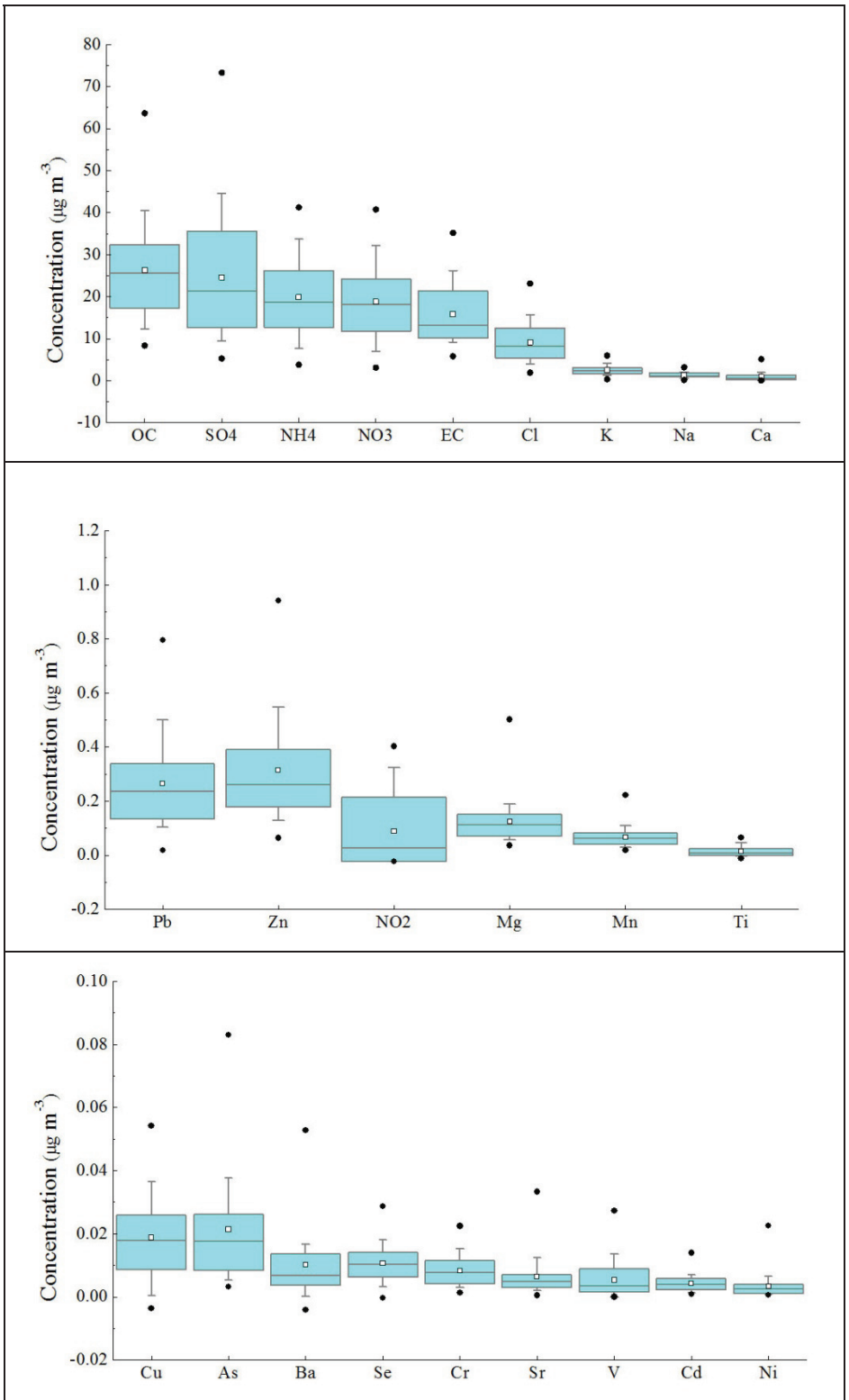


Figure 2. *The averaged concentrations for chemical components in $PM_{2.5}$ during Dec. 2012 to Jan. 2013. The bottom and top of the box represent the 25th and 75th percentile distribution for the component, respectively; the black line in the box represents the 50th percentile value; the ends of the whiskers represent the 10th and 90th percentile distribution for the corresponding component; the solid round represent minimum and the maximum value, respectively; the square in the box represents mean value of the component.*

OC and EC. The daily average concentrations of OC and EC were 26.3 μg m^{-3} and 15.8 μg m^{-3}, which accounted for 16.4% and 9.9% of $PM_{2.5}$ during this period, respectively. In January 1–13, the average concentrations of OC and EC were 38.6 μg m^{-3} and 20.1 μg m^{-3}, respectively. In January 14–31, the average concentrations of OC and EC were 26.1 μg m^{-3} and 11.6 μg m^{-3}, respectively. It was found that water–soluble ions and OC, EC presented different variations before and after the episode.

Elements in $PM_{2.5}$. The concentrations of measured trace elements are presented in Table 1. The order of concentrations for the elements were Zn>Pb>Mn>As>Cu>Ti>Ba>Se>Cr>Sr>V>Cd>Ni during this period. In comparison with the concentrations of these elements between January 1–13 and January 14–31, the results showed that the concentrations of Ba, Mn, Pb, Se, Sr, V and Zn in January 1–13 were higher than in January 14–31 period. The concentrations of other elements were higher during January 14–31.

3.2. The results of PMF analysis

As shown in Figure 3, the first factor was characterized by Ni, Cr and V, which were usually regarded as the marker components of fuel–oil combustion (Karnae and John, 2011; Yang et al., 2013). Therefore, this factor could be indentified as fuel–oil combustion. This source contributed 3.7 μg m^{-3} (2.5%) to $PM_{2.5}$.

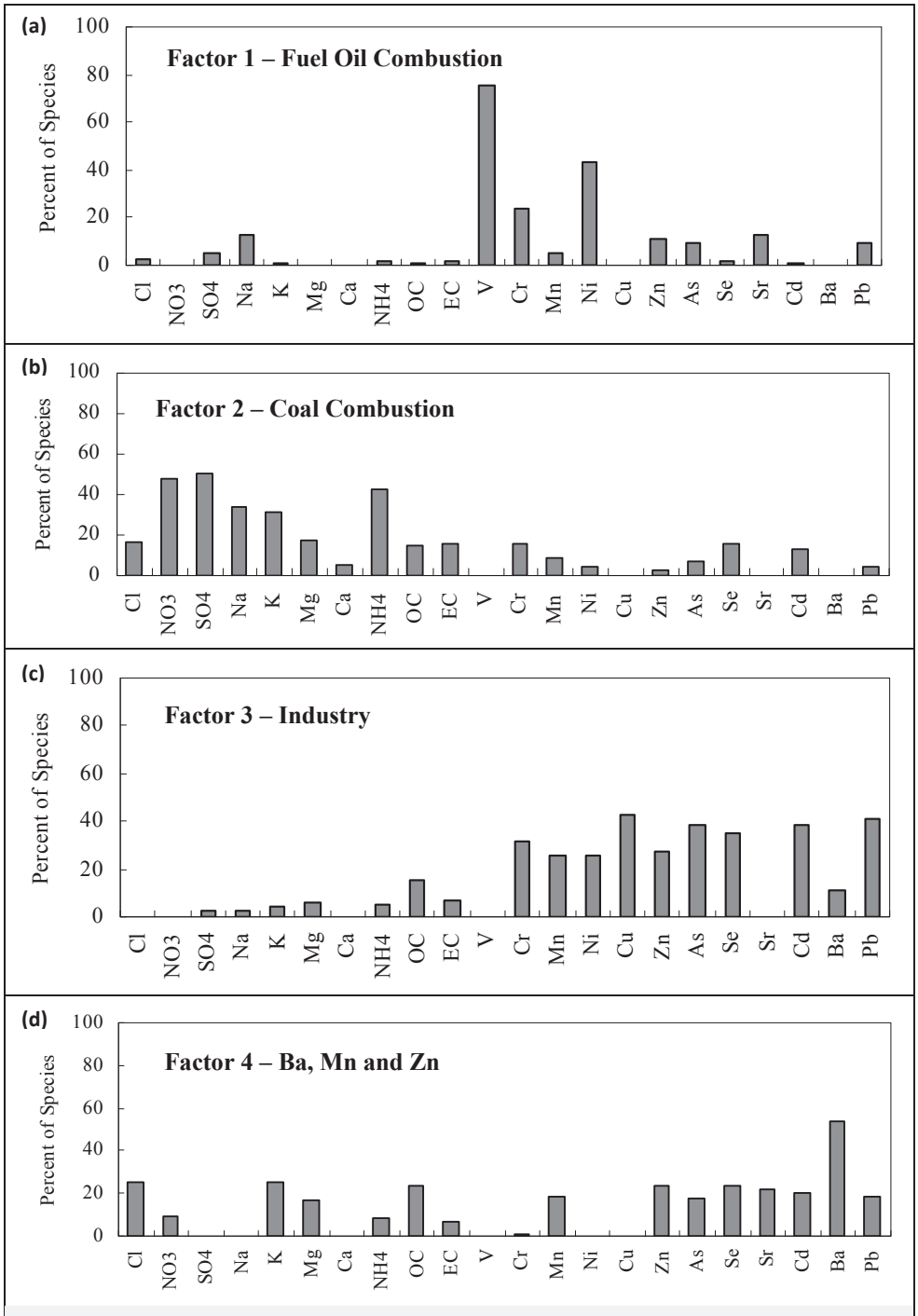


Figure 3. *Source profiles in EV values.* ***(a)*** *Factor 1–Fuel oil combustion,* ***(b)*** *Factor 2–Coal combustion,* ***(c)*** *Factor 3–Industry,* ***(d)*** *Factor 4–Ba, Mn and Zn,* ***(e)*** *Factor 5–K^+,As and V,* ***(f)*** *Factor 6–Secondary,* ***(g)*** *Factor 7–Motor vehicle,* ***(h)*** *Factor 8–Road dust.*

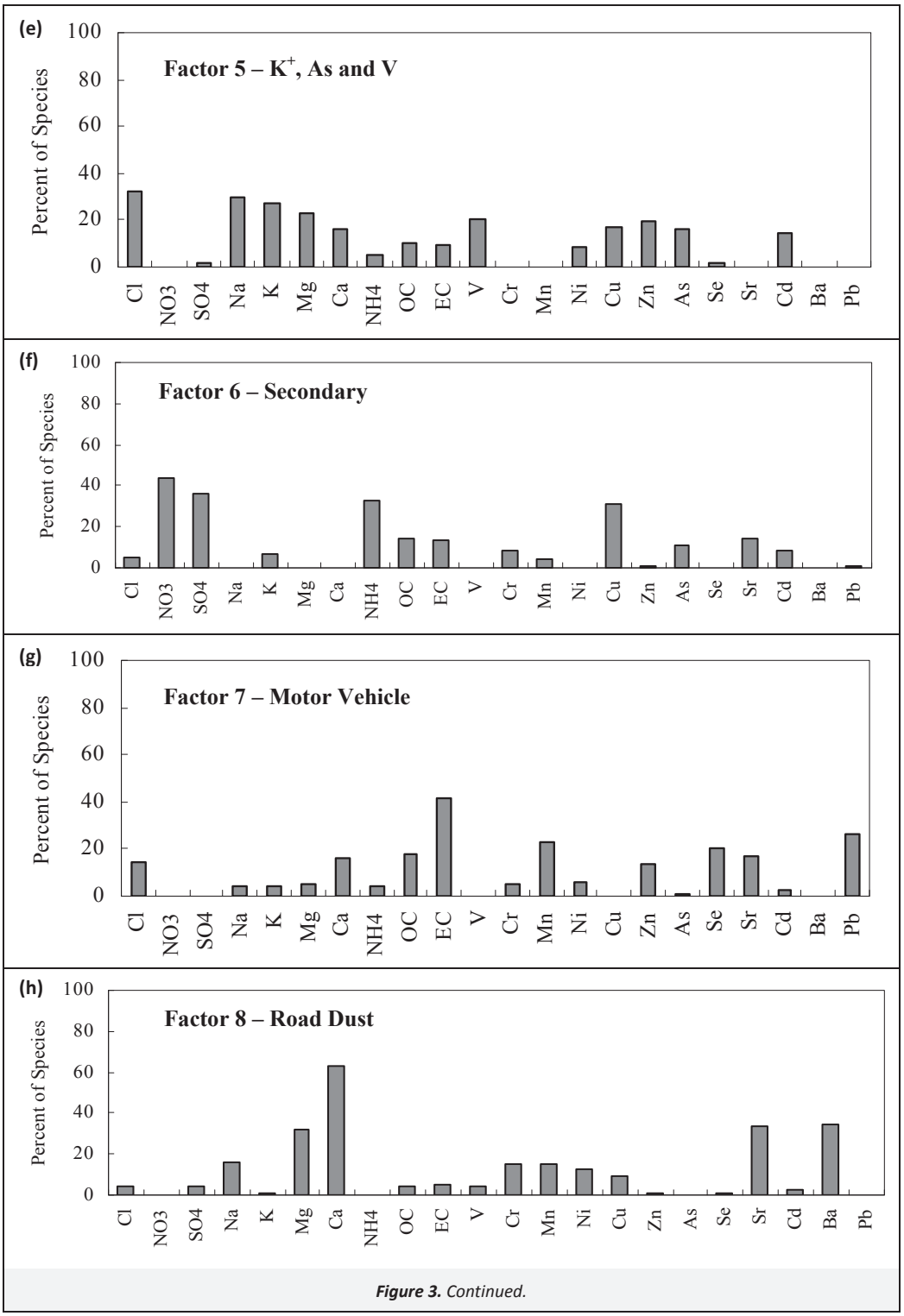


Figure 3. *Continued.*

The second factor might be identified as the coal combustion source. Because this factor had high loadings of NH_4^+, SO_4^{2-}, Na^+, K^+ and NO_3^- combined with the median loadings of Cl^-, OC, EC, Cr, Se and Cd. This source contributed 38.5 μg m^{-3} (25.9%) to $PM_{2.5}$. It was noted that the coal combustion was a major contributor to $PM_{2.5}$.

The third factor was characterized by high loadings of Cr, Mn, Ni, Cu, Zn, As, Se, Cd and Pb. V, Cr and Mn are closely associated with metal processing (Yu et al., 2013). Moreover, steel manufacturing located at western of Handan is a pillar industry. Zn and Pb are emitted primarily from the steel mills (Yang et al., 2013). This factor could be regarded as industry source, which contributed 24.1 μg m^{-3} (16.2%) to $PM_{2.5}$.

The factor 4 had tracer species of Cl^-, K^+, Mn, Zn, Se, Sr, Cd, Ba and Pb. These elements were quite common in number of source categories, including metal industry, biomass burning, waste incinerators and so on (Brown et al., 2007). Therefore, in this study, this factor was indentified as the Ba, Mn and Zn source, which contributed 18.9 μg m^{-3} (12.7%) to $PM_{2.5}$.

The fifth factor was similar to the fourth factor, and it should also be identified as a mixed source. Zn may be from waste

incinerator, While K^+ could be seen as a very important marker of biomass burning. oil combustion for industry and utilities was characterized by V and Ni, and As could be emitted from coal combustion. Even though these compositions come from different sources, they are produced by combustion. The fifth factor was named as K^+, As and V source. This factor contributed 9.3 μg m^{-3} (6.3%) to $PM_{2.5}$.

The sixth factor had high loadings of NH_4^+, SO_4^{2-} and NO_3^-. These ions, in the atmosphere, generated by the photochemical reaction of precursor gases (such as SO_2 and NO_X) emitted from coal combustion and motor vehicles. The sixth factor was thus regarded as the secondary source that contributed 32.5 μg m^{-3} (21.8%) to $PM_{2.5}$ on average.

The seventh factor was characterized by high loading of EC and moderate loadings, of Cl^-, Ca^{2+}, OC, Mn, Zn, Se, Sr and Pb. EC is emitted from the vehicle engines. Mn, Zn and Pb are typically related to the brake of the motor (Yang et al., 2013). In addition, Zn was a component of a common fuel detergent and anti–wear additive and could present the diesel emissions, as well as in tires, brake linings and pads (Brown et al., 2007). Ca^{2+} could be from the road dust. So the factor 7 was indentified as the motor source, which contributed 11.5 μg m^{-3} (7.7%) to $PM_{2.5}$.

The eighth factor was represented by not only Ca^{2+} but also the high loadings of Sr, Ba, Mg^{2+} and the median loadings of Cr, Mn, Ni and Cu. Metal sulfates (e.g., $CaSO_4$ and $MgSO_4$) can be formed when atmospheric H_2SO_4/SO_2 reacts with crustal aerosols. Cr, Mn, Ni and Cu were associated with tailpipe emissions, such as brake and tire wear (Yu et al., 2013). So the factor is regarded as the road dust source, which contributed 10.4 μg m^{-3} (6.9%) to $PM_{2.5}$ on average.

As shown in Table 2, the average predicted concentration of $PM_{2.5}$ by PMF was 149.0 μg m^{-3}, which was slightly lower than 160.1 μg m^{-3} of the measured concentration as shown in Table 1.

3.3. Chemical composition for visibility degradation B_{ext}

Visibility could be calculated by B_{ext} (unit in Mm^{-1}) with B_{ext}=1.9/visibility (Schichtel et al., 2001), where B_{ext} was extinction coefficient. B_{ext} was calculated by the concentration of chemical components as some researches mentioned, a IMPROVE Equation (5) was accepted and was used by other researches (Byun and Ching, 1999; Sister and Malm, 2000). In this Equation, Malm and Day (2001) proposed a relative humidity (RH) growth function *f*(RH), indicated how efficiencies increase for SO_4^{2-} and NO_3^- as they absorbed liquid water. (Table 3 gives the detailed value of *f* (RH)). Where, $(NH_4)_2SO_4$=4.125 [S]; NH_4NO_3=1.29 [NO_3^-]; POM (particulate organic matter)=1.4 [OC]; fine soil=2.2 [Al]+2.19 [Si] +1.63 [Ca]+2.42 [Fe]+1.94 [Ti]; coarse mass=[PM_{10}]–[$PM_{2.5}$]; 10 represents clear air scattering.

$$B_{ext} \approx 3\, f\,(\mathrm{RH})\,[(NH_4)_2SO_4+NH_4NO_3]+4\,[\mathrm{POM}]+10\,[\mathrm{EC}] +1\,[\text{fine soil}]+0.6\,[\text{coarse mass}]+10 \quad (5)$$

Considering that the fine soil, coarse mass and clear air scattering had little effect on the B_{ext} (Cheung et al., 2005). So this study used the equation as follows:

$$B_{ext} \approx 3\, f\,(\mathrm{RH})\,[(NH_4)_2SO_4+NH_4NO_3]+4\,[\mathrm{POM}]+10\,[\mathrm{EC}] \quad (6)$$

Figure 4 illustrated B_{ext} of four major chemical components during the different periods. The mean value of B_{ext} was 682.1 Mm^{-1} in this period. The highest contributor to B_{ext} was ammonium sulfate ranged from 26.5 Mm^{-1} to 635.2 Mm^{-1} with the mean value of 221.0 Mm^{-1} that accounted for 32.4% to the total B_{ext}, followed by 23.2% of EC (ranged from 58.2 Mm^{-1} to 352.0 Mm^{-1}), 22.8% of ammonium nitrate (ranged from 14.5 Mm^{-1} to 492.9 Mm^{-1}) and 21.6% of OC (ranged from 46.8 Mm^{-1} to 356.5 Mm^{-1}). The similar conclusion was that the biggest contributor of B_{ext} is ammonium sulfate reported in Jinan, in Guangzhou and in eastern United States (Sisler and Malm, 2000; Yang et al., 2007; Tao et al., 2009). Additionally, the mean values of B_{ext} were 582.2 Mm^{-1} and 802.0 Mm^{-1} in December and January, respectively. Comparison with December, all of B_{ext} of OC, ammonium nitrate and ammonium sulfate increased in January, while B_{ext} of EC decreased. A cause was that the absolute concentrations of OC, ammonium nitrate and ammonium sulfate increase, yet the concentration of EC decreased in January. In addition, for ammonium nitrate and ammonium sulfate, high relatively humidity could be auxiliary for enhancing B_{ext}. The mean relatively humidity was 76.2% in January, which was higher than 60.1% of December.

OC was the biggest contributor to B_{ext}, followed by EC, ammonium sulfate and ammonium nitrate in January 1–13. However, in January 14–31, ammonium sulfate ranked number one, followed by ammonium nitrate, OC and EC. That was also likely due to the increased concentrations of water–soluble ions and the higher RH in January 14–31. The RH increased from 54.3% of January 1–13 to 88.5% of January 14–31, respectively. Meanwhile, the *f*(RH) increased from 1.33 to 2.46.

4. Conclusion

The daily average concentration of $PM_{2.5}$ was 160.1 μg m^{-3} in Handan during December 1, 2012 to January 31, 2013. The water–soluble ions contributed 48.3% of $PM_{2.5}$. Almost a half of $PM_{2.5}$ suggested water–soluble ions were a major fraction in $PM_{2.5}$ in this period. The daily average concentration of January was 190.1 μg m^{-3}, which was higher than 135.1 μg m^{-3} of December. The higher proportion of December implied that the proportion of water–soluble ion didn't increase along with increase of absolute concentration of $PM_{2.5}$. The daily average concentrations of OC and EC were 26.3 μg m^{-3} and 15.8 μg m^{-3}, which accounted for 16.4% and 9.9% of $PM_{2.5}$ during this period, respectively.

In the extremely polluted period of January 1–13, the daily average concentration of $PM_{2.5}$ was 217.7 μg m^{-3}. However, the daily concentration of January 14–31 was only 139.5 μg m^{-3}. The proportion of the sum of SO_4^{2-}, NH_4^+ and NO_3^- in January 1–13 was 23.3%; yet the proportion of January 14–31 was 58.6%. It was found that SO_4^{2-}, NH_4^+ and NO_3^- presented lower concentrations in the early stage of the episode. The daily average concentrations of OC and EC were 38.6 μg m^{-3} and 20.1 μg m^{-3} in January 1–13, respectively. In January 14–31, the average concentrations of OC and EC were 26.1 μg m^{-3} and 11.6 μg m^{-3}, respectively. It was noted that the concentrations of OC and EC presented higher concentrations in the early stage of the episode than in the later of episode.

The predicted concentration of $PM_{2.5}$ was 149.0 μg m^{-3} applying PMF model, which was slightly lower than 160.1 μg m^{-3} of the measured concentration. Eight factors were identified by PMF method. They were coal combustion source, secondary source, industry source, Ba, Mn and Zn source, motor vehicle source, road dust source, K^+, As and V source, fuel oil combustion source, which contributed 25.9%, 21.8%, 16.2%, 12.7%, 10.9%, 7.7%, 6.3% and 2.5% of $PM_{2.5}$, respectively.

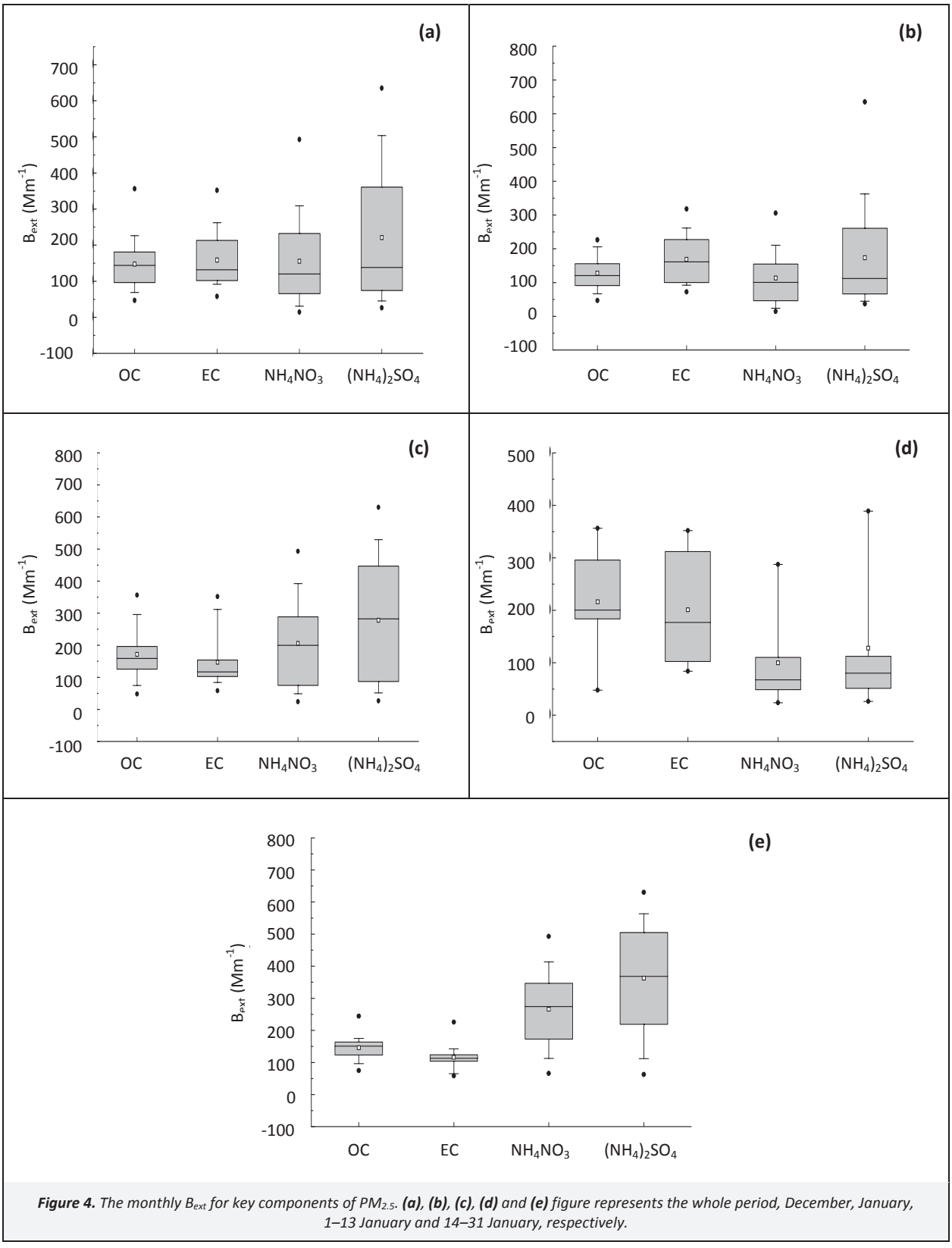


Figure 4. *The monthly B_{ext} for key components of $PM_{2.5}$.* ***(a), (b), (c), (d)*** *and* ***(e)*** *figure represents the whole period, December, January, 1–13 January and 14–31 January, respectively.*

The daily mean value of B_{ext} was 682.1 Mm^{-1} during this period. The daily mean value of B_{ext} ammonium sulfate was 221.0 Mm^{-1} which accounted for 32.4% of B_{ext}, followed by 24.9% of EC, 22.8%% of ammonium nitrate and 21.6% of OC. In January 1–13, OC was the biggest contributor for B_{ext}, followed by EC, ammonium sulfate and ammonium nitrate. However, in January 14–31, ammonium sulfate ranked number one, followed by ammonium nitrate, OC and EC. That was likely due to higher RH in January 14–31.

Acknowledgment

This study was sponsored by the National Natural Science Foundation of China (No. 41105105), the Natural Science Foundation of Hebei Province (No. D2011402019), the State Environmental Protection Key Laboratory of Sources and Control of Air Pollution Complex (No. SCAPC201307), the Excellent Young Scientist Foundation of Hebei Education Department (No. YQ2013031), the Program for the Outstanding Young Scholars of Hebei Province at HEBEU, China.

Table 2. *Mean source contributions to $PM_{2.5}$ components concentrations and percentages*

	Factor 1 [a]		Factor 2 [a]		Factor 3 [a]		Factor 4 [a]		Factor 5 [a]		Factor 6 [a]		Factor 7 [a]		Factor 8 [a]	
	Mass ($\mu g\ m^{-3}$)	Ratio (%)	Mass ($\mu g\ m^{-3}$)	Ratio (%)	Mass ($\mu g\ m^{-3}$)	Ratio (%)	Mass ($\mu g\ m^{-3}$)	Ratio (%)	Mass ($\mu g\ m^{-3}$)	Ratio (%)	Mass ($\mu g\ m^{-3}$)	Ratio (%)	Mass ($\mu g\ m^{-3}$)	Ratio (%)	Mass ($\mu g\ m^{-3}$)	Ratio (%)
$PM_{2.5}$	3.7	2.5	38.5	25.9	24.1	16.2	18.9	12.7	9.3	6.3	32.5	21.8	11.5	7.7	10.4	7.0
OC	0.1	0.5	3.7	14.9	3.8	15.3	5.8	23.6	2.4	9.8	3.4	14.0	4.4	17.8	1.0	4.1
SO_4^{2-}	1.2	5.4	11.5	50.4	0.5	2.2	0	0	0.5	2.0	8.2	35.9	0	0	0.9	4.0
NH_4^+	0.3	1.8	8.4	42.3	1.0	5.2	1.7	8.6	1.0	5.2	6.5	32.7	0.8	4.2	0	0
NO_3^-	0	0	8.8	47.5	0	0	1.7	9.0	0	0	8.1	43.5	0	0	0	0
EC	0.2	1.4	2.3	15.6	1.1	7.0	1.0	6.8	1.4	9.4	2.0	13.2	6.2	41.6	0.8	5.1
Cl^-	0.2	2.4	1.4	16.2	0	0	2.2	25.0	2.8	32.3	0.4	5.1	1.3	14.6	0.4	4.4
K^+	0	0.9	0.7	31.5	0.1	4.4	0.6	25.4	0.6	26.7	0.2	6.6	0.1	3.9	0	0.6
Na^+	0.2	13.0	0.4	34.0	0.04	2.9	0	0	0.4	30.0	0	0	0.06	4.4	0.2	15.7
Ca^{2+}	0	0	$48.5x10^{-3}$	5.5	0	0	0	0	$141.9x10^{-3}$	16.0	0	0	$139.4x10^{-3}$	15.8	$554.6x10^{-3}$	62.7
Pb	$24.8x10^{-3}$	9.7	$11.7x10^{-3}$	4.6	$105.4x10^{-3}$	41.0	$46.9x10^{-3}$	18.3	0	0	$1.6x10^{-3}$	0.6	$66.5x10^{-3}$	25.9	0	0
Zn	$31.4x10^{-3}$	11.1	$8.0x10^{-3}$	2.8	$77.9x10^{-3}$	27.6	$67.0x10^{-3}$	23.7	$55.4x10^{-3}$	19.6	$2.2x10^{-3}$	0.8	$39.2x10^{-3}$	13.9	$1.5x10^{-3}$	0.5
Mg^{2+}	0	0	$21.5x10^{-3}$	17.7	$7.8x10^{-3}$	6.4	$20.0x10^{-3}$	16.5	$27.8x10^{-3}$	22.9	$0.1x10^{-3}$	0.1	$5.8x10^{-3}$	4.8	$38.3x10^{-3}$	31.6
As	$1.6x10^{-3}$	8.9	$1.3x10^{-3}$	7.0	$7.0x10^{-3}$	38.7	$3.2x10^{-3}$	17.4	$3.0x10^{-3}$	16.3	$1.9x10^{-3}$	10.7	$0.2x10^{-3}$	1.0	0	0
Ba	0	0	0	0	$1.2x10^{-3}$	11.5	$5.4x10^{-3}$	53.7	0	0	0	0	0	0	$3.5x10^{-3}$	34.8
Cd	0	0.9	$0.5x10^{-3}$	13.0	$1.5x10^{-3}$	38.3	$0.8x10^{-3}$	20.2	$0.6x10^{-3}$	14.3	$0.3x10^{-3}$	8.1	$0.1x10^{-3}$	2.8	$0.1x10^{-3}$	2.3
Cr	$1.8x10^{-3}$	23.4	$1.2x10^{-3}$	15.3	$2.5x10^{-3}$	31.9	$0.1x10^{-3}$	0.9	0	0	$0.7x10^{-3}$	8.5	$0.4x10^{-3}$	5.0	$1.2x10^{-3}$	14.9
Cu	0	0	0	0	$8.3x10^{-3}$	43.1	0	0	$3.2x10^{-3}$	16.8	$6.0x10^{-3}$	31.1	0	0	$1.7x10^{-3}$	9.0
Mn	$3.2x10^{-3}$	5.0	$5.6x10^{-3}$	8.8	$16.1x10^{-3}$	25.4	$11.8x10^{-3}$	18.6	0	0	$2.4x10^{-3}$	3.8	$14.7x10^{-3}$	23.1	$9.7x10^{-3}$	15.2
Ni	$1.2x10^{-3}$	43.2	$0.1x10^{-3}$	4.3	$0.7x10^{-3}$	25.6	0	0	$0.2x10^{-3}$	8.5	0	0	$0.2x10^{-3}$	5.9	$0.3x10^{-3}$	12.5
Se	$0.2x10^{-3}$	1.8	$1.6x10^{-3}$	16.1	$3.6x10^{-3}$	35.4	$2.4x10^{-3}$	23.8	$0.2x10^{-3}$	1.5	0	0	$2.1x10^{-3}$	20.4	$0.1x10^{-3}$	1.0
Sr	$0.7x10^{-3}$	12.8	0	0	0	0.3	$1.2x10^{-3}$	21.9	0	0	$0.8x10^{-3}$	14.3	$0.9x10^{-3}$	17.1	$1.8x10^{-3}$	33.8
V	$3.9x10^{-3}$	75.2	0	0	0	0	0	0	$1.1x10^{-3}$	20.2	0	0.4	0	0	$0.2x10^{-3}$	4.2
Source	Fuel oil combustion		Coal combustion		Industry		Ba, Mn and Zn		K^+, As and V		Secondary		Motor vehicle		Road dust	

[a] *Ratio is the concentration of one factor accounts for the concentration of all of these factors*

Table 3. *Statistical summary of mean f(RH) values in selected relative humidity ranges*

RH(%)	f(RH)
30~35	1.16
35~40	1.21
40~45	1.22
45~50	1.27
50~55	1.33
55~60	1.38
60~65	1.45
65~70	1.55
70~75	1.65
75~80	1.83
80~85	2.10
85~90	2.46
>90	3.17

References

Brown, S.G., Frankel, A., Raffuse, S.M., Roberts, P.T., Hafner, H.R., Anderson, D.J., 2007. Source apportionment of fine particulate matter in Phoenix, AZ, using positive matrix factorization. *Journal of the Air & Waste Management Association* 57, 741–752.

Byun, D. W., Ching J. K. S., 1999. Science Algorithms of the EPA Models–3 Community Multiscale Air Quality (CMAQ) Modeling System, EPA/600/R–99/030.

Cheung, H.C., Wang, T., Baumann, K., Guo, H., 2005. Influence of regional pollution outflow on the concentrations of fine particulate matter and visibility in the coastal area of Southern China. *Atmospheric Environment* 39, 6463–6474.

Chueinta, W., Hopke, P.K., Paatero, P., 2000. Investigation of sources of atmospheric aerosol at urban and suburban residential areas in Thailand by positive matrix factorization. *Atmospheric Environment* 34, 3319–3329.

Dunker, A.M., Morris, R.E., Pollack, A.K., Schleyer, C.H., Yarwood, G., 1996. Photochemical modeling of the impact of fuels and vehicles on urban ozone using auto oil program data. *Environmental Science & Technology* 30, 787–801.

Karnae, S., John, K., 2011. Source apportionment of fine particulate matter measured in an industrialized coastal urban area of south Texas. *Atmospheric Environment* 45, 3769–3776.

Kim, E., Hopke, P., 2008. Source characterization of ambient fine particles at multiple sites in the Seattle area. *Atmospheric Environment* 42, 6047–6056.

Lee, E., Chan, C.K., Paatero, P., 1999. Application of positive matrix factorization in source apportionment of particulate pollutants in Hong Kong. *Atmospheric Environment* 33, 3201–3212.

MEP (Ministry of Environmental Protection), 2012. China National Ambient Air Quality Standards, GB3095–2012.

Malm, W.C., Day, D.E., 2001. Estimates of aerosol species scattering characteristics as a function of relative humidity. *Atmospheric Environment* 35, 2845–2860.

Paatero, P., 1997. Least squares formulation of robust non–negative factor analysis. *Chemometrics and Intelligent Laboratory Systems* 37, 23–35.

Paatero, P., Tapper, U. 1994. Positive matrix factorization: a non–negative factor model with optimal utilization of error estimates of data values. *Environments* 5, 111–126.

Qin, Y.J., Kim, E., Hopke, P.K., 2006. The concentrations and sources of $PM_{2.5}$ in metropolitan New York City. *Atmospheric Environment* 40, S312–S332.

Schichtel, B.A., Husar, R.B., Falke, S.R. and Wilson, W.E., 2001. Haze trends over the United States, 1980–1995. *Atmospheric Environment* 35, 5205–5210.

Sister, J.F., Malm, W.C., 2000. Interpretation of trends of $PM_{2.5}$ and reconstructed visibility from the improve network. *Journal of the Air & Waste Management Association* 50, 775–789.

Tao, J., Ho, K.F., Chen, L.G., Zhu, L.H., Han, J.L., Xu, Z.C., 2009. Effect of chemical composition of $PM_{2.5}$ on visibility in Guangzhou, China, 2007 spring. *Particuology* 7, 68–75.

U.S. EPA (U.S. Environmental Protection Agency), 2008. EPA Positive Matrix Factorization (PMF) 3.0 Fundamentals & User Guide.

Wang, L.T., Wei, Z., Yang, J., Zhang, Y., Zhang, F.F., Su, J., Meng, C.C., Zhang, Q., 2014. The 2013 severe haze over southern Hebei, China: Model evaluation, source apportionment, and policy implications. *Atmospheric Chemistry and Physics* 14, 3151–3173.

Wang, L.T., Xu, J., Yang, J., Zhao, X.J., Wei, W., Cheng, D.D., Pan, X.M., Su, J., 2012. Understanding haze pollution over the southern Hebei area of china using the CMAQ model. *Atmospheric Environment* 56, 69–79.

Wei, Z., Yang, J., Wang, L T., Wei, W., Zhang, F F. and Su, J., 2014. Characteristics of the severe haze episode in Handan city in January, 2013. *Environmental Science & Technology* (In Chinese) (Article in Press).

Wei, W., Wang, L. T., Pan, X. M., Cheng, D. D. and Su, J., 2013. Simulation study of haze pollution sources in cities of Hebei Province. *Environmental Science & Technology* 36, 116–119 (In Chinese).

Yang, L.X., Cheng, S.H., Wang, X.F., Nie, W., Xu, P.J., Gao, X.M., Yuan, C., Wang, W.X., 2013. Source identification and health impact of $PM_{2.5}$ in a heavily polluted urban atmosphere in China. *Atmospheric Environment* 75, 265–269.

Yang, L.X., Wang, D.C., Cheng, S.H., Wang, Z., Zhou, Y., Zhou, X.H., Wang, W.X., 2007. Influence of meteorological conditions and particulate matter on visual range impairment in Jinan, China. *Science of the Total Environment* 383, 164–173.

Yu, L.D., Wang, G.F., Zhang, R.J., Zhang, L.M., Song, Y., Wu, B.B., Li, X.F., An, K., Chu, J.H., 2013. Characterization and source apportionment of $PM_{2.5}$ in an urban environment in Beijing. *Aerosol and Air Quality Research* 13, 574–583.